Polymer Bulletin (2023) 80:2367–2387
https://doi.org/10.1007/s00289-022-04143-z

ORIGINAL PAPER

Poly(vinyl alcohol) membranes-inspired heterocyclic compounds for different applications: synthesis and characterization

Nadia G. Kandile[1] · **Abir S. Nasr**[1]

Received: 23 April 2021 / Revised: 25 January 2022 / Accepted: 9 February 2022 /
Published online: 11 March 2022

Abstract

Chemical modification of poly(vinyl alcohol) (PVA) with different monomers is a convention method for the development of its properties. In this study, the new multifunctional membranes $(PVA\text{-}A)_{1-3}$, $(PVA\text{-}P)_{1-3}$, (PVA-AG) and (PVA-PG) were designed and synthesized by the reaction of PVA with heterocyclic compounds [*N*,*N*′-bi-*α*-azido succinimide (A), *N*-phthalimido-*α*-azido succinimide (P)] and using glutaraldehyde (G) as cross-linker, respectively. The new membranes were characterized by FT-IR, TGA, SEM and X-ray diffraction. The swelling behavior of the membranes showed that membranes $(PVA\text{-}P)_{1-3}$ exhibited the highest swelling capacity in different solvents. Their antibacterial against (Gram-negative), (Gram-positive) bacteria, and in vitro drug loading and release activities were evaluated. Additionally, metal ions adsorption capacity for copper, cobalt and mercury ions was studied. (PVA-AG) membrane performed the highest inhibitory effect to *E. coli*, *Proteus*, *S. aureus* and *B. subtilis* bacteria reached 22.9, 25.46, 24.9 and 30.56, respectively. Furthermore, in vitro controlled loading and release of lidocaine, $(PVA\text{-}A)_1$ membrane revealed remarkable ability reached 57.37% and 94.59%, respectively. Hydrogel (PVA-AG) showed the highest metal ions (copper, cobalt and mercury) uptake efficiency (64.5, 69.5 and 73), respectively. Based on results, the prepared membranes can be suggested as promising agents for antibacterial, drug delivery systems and metal ions removal from aqueous medium.

Keywords PVA membranes · Antibacterial · Drug carriers · Heterocyclic compounds · Metal ions adsorption

✉ Abir S. Nasr
abirsnasr@yahoo.com

[1] Chemistry Department, Faculty of Women for Arts, Science and Education, Ain Shams University, Heliopolis, Cairo 11757, Egypt

Introduction

Poly(vinyl alcohol) (PVA) is the largest synthetic water-soluble and semicrystalline polymer produced in the world [1, 2]. Due to its unique characteristics involving processability, hydrophilicity biocompatibility, film forming ability, nontoxicity, biodegradability and barrier properties, PVA is used in a wide range of applications such as fibers, films, membranes, materials for drug delivery system, biocompatible glucose sensor [3], water treatment [4] and antibacterial activity [5–9]. It is a polymer of large attention because of its various desired characteristics specifically for pharmaceutical and biomedical applications [10–12].

The modification of PVA is needed to destroy its intermolecular and intramolecular interactions that exits between hydroxyl groups on its molecular chains, and it reacts with other polymers due to its hydrophilicity [1, 13].

Cross-linking of PVA is used to produce different types of polymers which presents a broad range of applications in industry [14–16]. Dialdehydes, such as glyoxal [17] or glutaraldehyde [18], are the most commonly used cross-linkers for PVA. The highly multilateral chemical cross-linking is used to modify polymers, to enhance its properties, such as mechanical, chemical and thermal stability [19, 20]. PVA hydrogel can be used as adsorbent. The adsorption efficiency of Cu^{2+} onto PVA hydrogel adsorbents with several cross-linking degrees from aqueous solution indicated that PVA formed cross-linked hydrogel with glutaraldehyde have uptake ratio in the range of 195–250% [21]. PVA is modified with chitosan (CS) in the presence of calcium chloride ($CaCl_2$) to form cross-linking membranes with more flexibility than a CS-PVA membrane itself and can be used for biomedical applications [22]. In addition, chitosan/polyvinyl alcohol blend can form a good antibacterial membrane for air filtration [23].

Several researchers have modified the PVA by introducing interactive functional groups such as carboxylic, sulfonate and amino groups because they believe it is essential to expand the application potential of modified PVA [24, 25]. Preparation of PVA containing phosphorus and heteroaromats in the polymer chain has attracted the attention of many researchers because of the excellence in their properties such as the susceptibility to inflammation, high melting points, thermal stability and extraction of heavy metal ions [26, 27]. Interpenetrating network (IPN) can be formed by chemical modifications of poly(vinyl alcohol) with several heterocyclic compounds which improve the antibacterial effectiveness of the resulting polymers against 2 types of bacteria [28].

Recently, interpenetrating network (IPN) and semi-IPN polymer structures can be used for releasing drugs in a controlled manner [29], as example, blend microspheres of cellulose triacetate and bee wax are used for investigating the controlled release of nateglinide, an antidiabetic drug with a plasma half-life of 1.5 h [30].

Bismaleimides (BMI) have been employed as chain extenders, and cross-linking agents with many polymers and composite systems. The thermal properties of bismaleimide polymers were affected by the length of the main carbon chain on it. The BMI system is influenced by the chemical nature of the maleimide

rings. The presence of BMI in the modified polymers possesses the capability of membrane-forming [31, 32].

This study is extension of our previous work for the preparation of new modified polymers for different applications [33–38], polyvinyl alcohol was taken as the basic matrix and modified with two heterocyclic compounds [*N*,*N*′-bi-*α*-azido succinimide (A) and *N*-phthalimido-*α*-azido succinimide (P)] via their reaction in the absence or presence of glutaraldehyde as a cross-linker to enhance the physicochemical properties of PVA. The prepared membranes were characterized using FTIR spectrum, X-ray, thermal analysis (TGA) and scanning electron microscopy (SEM). Also, antibacterial activity, drug loading and release and metal ions adsorption from aqueous medium for the membranes were investigated.

Experimental

Chemicals and reagents

Poly(vinyl alcohol) (PVA): 88% hydrolyzed powder average M.W = 10 k Da (Aldrich), 10% PVA solution was prepared by gentle heating of 10 gm PVA in 100 ml distilled water, glutaraldehyde (25 wt% in H_2O) (Aldrich), pyridine (Merck), maleic anhydride (EL Nasr Pharmaceutical Chemicals Co.) (Egypt), phthalic anhydride (Aldrich), acetic anhydride (Fluka), hydrazine hydrate (99%) (Alpha), sodium carbonate (EL Nasr Pharmaceutical Chemicals Co.) (Egypt), glacial acetic acid, dimethyl sulfoxide, sodium azide (Aldrich), methanol (Alpha), benzene, dimethylformamide (Adwic), lidocaine, copper sulfate (Aldrich), cobalt acetate (Aldrich) and mercuric chloride (Aldrich), *N*,*N*′-bi-*α*-azido succinimide (A) was prepared according to Awad et al. [39], *N*-phthalimido-α-azido succinimide (P) was prepared according to Awad et al. [40].

Instrumental analysis

Melting points were illustrated by a Boetius device.

The thickness of membranes was measured using SOMET 0–25/0.01 mm Micrometer (CSN 251420).

FTIR spectra were determined by PerkinElmer-1430, using the KBr Wafer technique.

X-ray diffraction was carried out with a Phillips X-ray (Generator PW-1390) with a Ni-filtered Cu Kα radiation source ($\lambda = 0.154$ nm), set at scan rate = 10°/min, using a voltage of 40 kv and a current of 30 mA was for measuring the diffraction patterns of the membrane. The sample was ground well and scanned at 2θ range from 4° to 90°.

Thermal analysis (TGA) was measured in a nitrogen atmosphere by a Shimadzu TGA-50H thermal analyzer.

The morphology was determined by scanning electron microscopy using Model JXA 850 prop microanalyzer. The samples were mounted on a metal stub with

double stick adhesive tape and coated under vacuum with gold. The gold film thickness was 150 Å. The scanning occurred at accelerating voltage 30 kV and magnification at 30 × 4000 µm, at 50 × 2000 µm and at 100 × 1000 µm.

Methods

Membranes preparation

Modification of poly(vinyl alcohol) with *N,N′*-bi-*α*-azido succinimide (A) and *N*-phthalimido-*α*-azido succinimide (P).

A mixture of *N*,*N*′-bi-*α*-azido succinimide (A) or *N*-phthalimido-*α*-azido succinimide (P) at different concentrations (0.5 mmol, 1.5 mmol and 2.5 mmol), (10 ml) of 10% PVA solution and pyridine (0.2 ml) was refluxed for 1 h with stirring. The reaction mixture was poured into petri dish and left at room temperature until complete solvent evaporation to form the membranes. The membranes were washed with dimethylformamide and dried in oven at 100 °C for 30 min. to give: $(PVA\text{-}A)_{1–3}$ and $(PVA\text{-}P)_{1–3}$, respectively. The thickness of the prepared membranes was (180, 190, 210) µm and (150, 170, 190) µm, respectively.

Modification of poly(vinyl alcohol) with *N,N′*-bi-*α*-azido succinimide (A) and *N*-phthalimido-*α*-azido succinimide (P) in the presence of glutaraldehyde.

A mixture of *N*,*N*′-bi-*α*-azido succinimide (A) or *N*-phthalimido-*α*-azido succinimide (P) (0.5 mmol), (10 ml) of 10% PVA solution, (25%, 5 ml) glutaraldehyde and pyridine (0.2 ml) was refluxed with stirring until complete gelation. The reaction mixture was poured into petri dish and left at room temperature until complete solvent evaporation to form the membranes. The membranes were washed with dimethylformamide and dried in oven at 100 °C for 30 min. to give: (PVA-AG) and (PVA-PG), respectively. The thickness of the prepared membranes was 240 µm and 230 µm, respectively.

Characterization of the prepared membranes

Determination of sol–gel fraction

The soluble and gel fraction were determined gravimetrically, a constant weight (W_0) of membranes $(PVA\text{-}A)_{1–3}$, $(PVA\text{-}P)_{1–3}$, (PVA-AG) and (PVA-PG) were placed in 20 ml of different solvents as [distilled water, methanol, dimethylformamide and dimethylsulfoxide] and then boiled for 1 h. The swelled pieces of the membrane samples were taken and dried in oven at 120 °C to remove the excess of the solvent. Drying to constant weight (W_1) was obtained. The soluble and gel fraction was calculated according to the following equations [41]:

$$\text{Soluble fraction (SF\%)} = \frac{W_0 - W_1}{W_0} \times 100 \tag{1}$$

where W_0 is the initial weight of the membrane, W_1 is the weight of dried membrane after removal of the solvent.

$$\text{Gel fraction (\%)} = 100 - \text{Sol fraction.} \tag{2}$$

Determination of swelling ratio

The swelling ratio was determined gravimetrically, a certain weight (W_1) of the membrane was soaked in 20 ml of different solvents [distilled water, methanol, dimethylformamide and dimethylsulfoxide] for 24 h at room temperature. The sample was removed from the beaker and blotted with a filter paper just to remove the droplet of solvents on the surface.

The swelling ratio was calculated according to the following equation [42]:

$$\text{Swelling ratio (\%)} = \frac{W_2 - W_1}{W_1} \times 100 \tag{3}$$

where W_1 is the weight of dry membrane, W_2 is the weight of the swollen membrane.

The swelling ratio experiments were repeated three times and the results are expressed as the mean ± standard deviation (SD).

Drug loading and release

The membranes were equilibrated in 1000 ppm (mg/L) of lidocaine (LD) prepared in phosphate buffer at pH 7.4 at room temperature for 2 days. After loading, the membranes were removed from the solution and rinsed with buffer solution, then calculated the weight of the (LD) taken by the membranes.

The lidocaine (LD) releases occur by immersing the loaded (LD) membranes in a vessel containing 10 ml of phosphate buffer pH 7.4 at room temperature with shaking, then calculate the weight of the released (LD). The amount of drug loaded in membranes and the percentage release of the (LD) were determined by the following equations [43, 44]:

$$\text{\% Drug loading} = \frac{W_D - W_d}{W_d} \times 100 \tag{4}$$

$$\text{\% Release} = \frac{W_t}{W_D} \times 100 \tag{5}$$

where W_d is the weight of dried membranes before immersion in the drug solution, W_D is the weight of dried membranes after immersion in the drug solution, W_t is the weight of the released lidocaine (LD).

Both drug loading and release experiments were repeated three times and the results are expressed as the mean ± SD.

Evaluation of the efficiency of metal ions uptake

To determine the metal ions uptake from aqueous solution [copper sulfate, cobalt acetate and mercuric chloride] (0.05 g in 25 ml water), the prepared membranes were preswelled in water until constant weights were obtained. The preswelled membranes were immersed in the solution for 5 h and10 h. The absorbance of M^{2+}ions was measured at different time periods using UV–visible spectrometry.

The efficiency of metal uptake of the investigated membranes was calculated using the following equation [36]:

$$F(\%) = \left[1 - \frac{C}{C_0}\right] \times 100 \tag{6}$$

where F is efficiency (%), C is the concentration of M^{2+}in the solution after a certain time, C_0 is the initial concentration of M^{2+}solution.

Results and discussion

Modification of poly(vinyl alcohol) with different heterocyclic compounds (A) and (P)

The aim of our research is the preparation of new membranes by chemical modification of poly(vinyl alcohol) with functionalized groups of heterocyclic compounds [*N*,*N*′-bi-*α*-azido succinimide (A) and *N*-phthalimido-*α*-azido succinimide (P)] at 3 different concentrations via the nucleophilic attack of hydroxyl groups of PVA on the carbonyl groups of heterocyclic compounds via ring-opening to give new membranes $(PVA\text{-}A)_{1–3}$ and $(PVA\text{-}P)_{1–3}$, respectively, to study the effect of the different concentrations of the monomers (A) and (P) on the properties of the prepared membranes. However, chemical modifications of PVA with (A) and (P) in the presence of glutaraldehyde as cross-linker were performed to give the membranes (PVA-AG) and (PVA-PG), respectively (Scheme 1).

Characterization of the prepared membranes

The new membranes were characterized by FTIR, thermogravimetric analysis (TGA), X-ray diffraction and scanning electron microscopy (SEM).

Fourier transforms infrared (FTIR) spectroscopy

The FTIR spectra were used to study the structures of PVA and the membranes $(PVA\text{-}A)_1$, $(PVA\text{-}P)_1$, (PVA-AG) and (PVA-PG). The FTIR spectra of the new

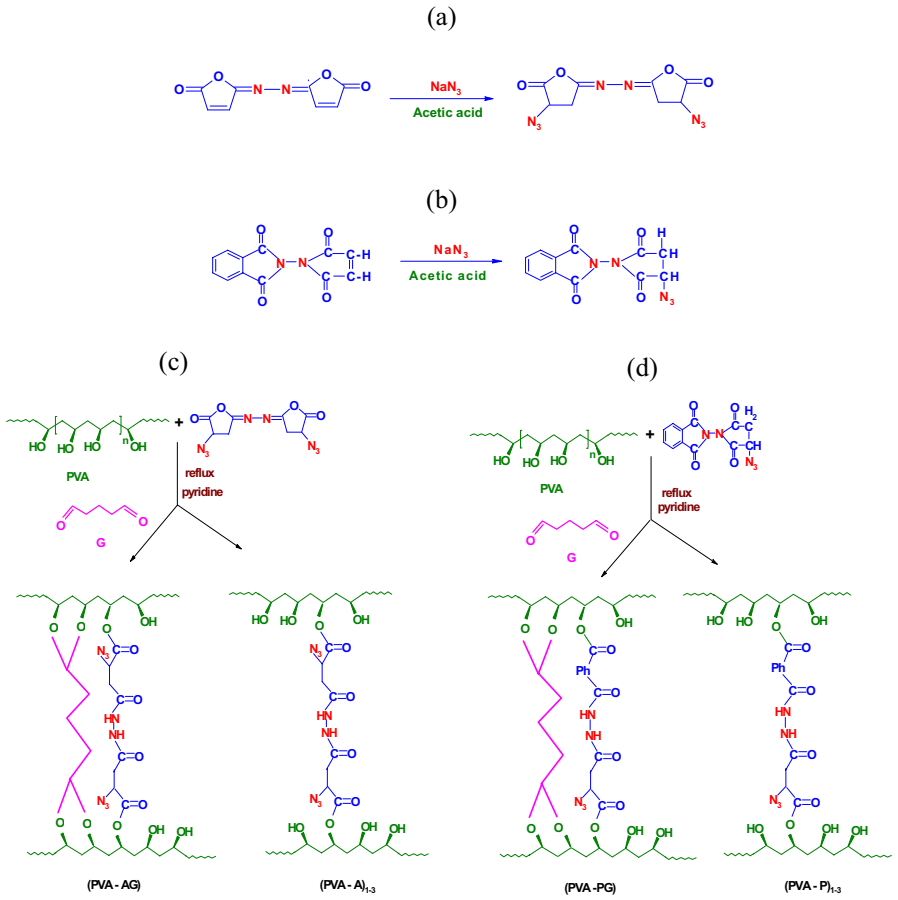

Scheme 1 Synthesis of **a** *N*,*N*′-bi-*α*-azido succinimide, **b** *N*-phthalimido-*α*-azido succinimide, **c** (PVA-A)$_{1-3}$ and (PVA-AG) and **d** (PVA-P)$_{1-3}$ and (PVA-PG)

membranes showed ester formation between the hydroxyl groups of the PVA chains and the carbonyl groups of heterocyclic compounds (A) and (P). FTIR spectra of the membranes showed characteristic absorption bands at 1741–1746 cm^{-1} assigned for carbonyl group stretching, and at 2110–2113 cm^{-1} assigned for azide group, peaks at 2922–2924 cm^{-1} for (CH) stretching of (CH_2) group and absorption bands at 3428–3446 cm^{-1} for (OH) of PVA implies for N–H stretching of heterocyclic compounds. The characteristic absorption bands for membranes prepared in the presence of glutaraldehyde showed absorption bands at 1103, 1153 cm^{-1} assigned for aliphatic ether (C–O–C) stretching resulted from reaction of PVA with glutaraldehyde and formation of acetal [45] as shown in Fig. 1.

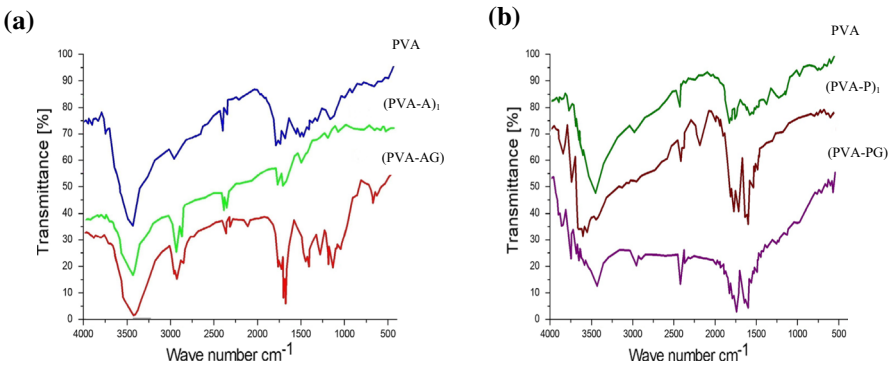

Fig. 1 Infrared spectra of **a** PVA, $(PVA\text{-}A)_1$, (PVA-AG) and **b** PVA, $(PVA\text{-}P)_1$, (PVA-PG)

Thermogravimetric analysis (TGA)

The thermal stability of the membranes was evaluated by TGA in air at a heating rate of 10 °C/min. PVA showed three main weight loss stages, the first stage at 170 °C attributed to evaporate strong bound water, the second stage at 300 °C that indicated the dehydration reaction on the polymer chain, and the 3rd stage at around 400–480 °C due to the decomposition of the polymer [46–48]. The thermograph of the membranes showed that the weight loss of the cross-linked membranes in low temperature around (167–180 °C) may be indicated to the ease of degradation of multifunctional groups; however, the weight loss in the high temperature around (324–449 °C) due to the degradation of the main chain of the polymers (Fig. 2). The results showed that the thermal stability for membranes (PVA-AG) and (PVA-PG) was improved attributed to the increase in degree of cross-linking due to the cross-linking with glutaraldehyde.

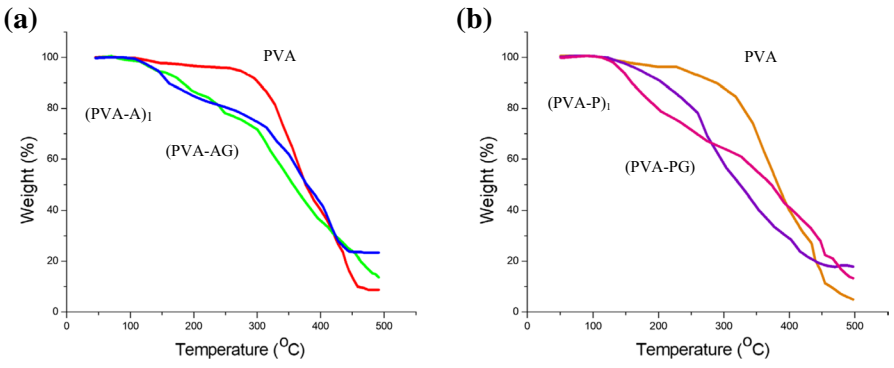

Fig. 2 TGA for **a** PVA, $(PVA\text{-}A)_1$, (PVA-AG) and **b** PVA, $(PVA\text{-}P)_1$, (PVA-PG)

X-ray diffraction

X-ray diffraction analysis is used to investigate the crystalline structure of the membranes. The X-ray diffraction of the new membranes exhibited lower intensity peaks than PVA. The new membranes showed that the crystallinity of the prepared membranes decreases with increasing the concentration of the monomers (A) and (P) in the membranes $(PVA\text{-}A)_{1–3}$ and $(PVA\text{-}P)_{1–3}$ [49]. This result was due to the increasing of the degree of cross-linking in the membranes as shown in Fig. 3a, b. The interfering peaks at 2θ in the range $4–90^0$ indicated the intermediate properties of membranes between crystalline and amorphous properties. Additionally, increase in the peaks height of the X-ray diffraction of membranes (PVA-AG) and (PVA-PG) in the presence of cross-linking glutaraldehyde indicated increase in crystallinity than the membranes formed in the absence of glutaraldehyde due to thickness increase in the cross-linking membrane (Fig. 3c, d) [50].

Solubility

The solubility of the prepared membranes $(PVA\text{-}A)_{1–3}$, $(PVA\text{-}P)_{1–3}$, (PVA-AG) and (PVA-PG) was studied in different solvents at room temperature. Although PVA is water soluble, the new membranes were insoluble in the different solvents as: DMF,

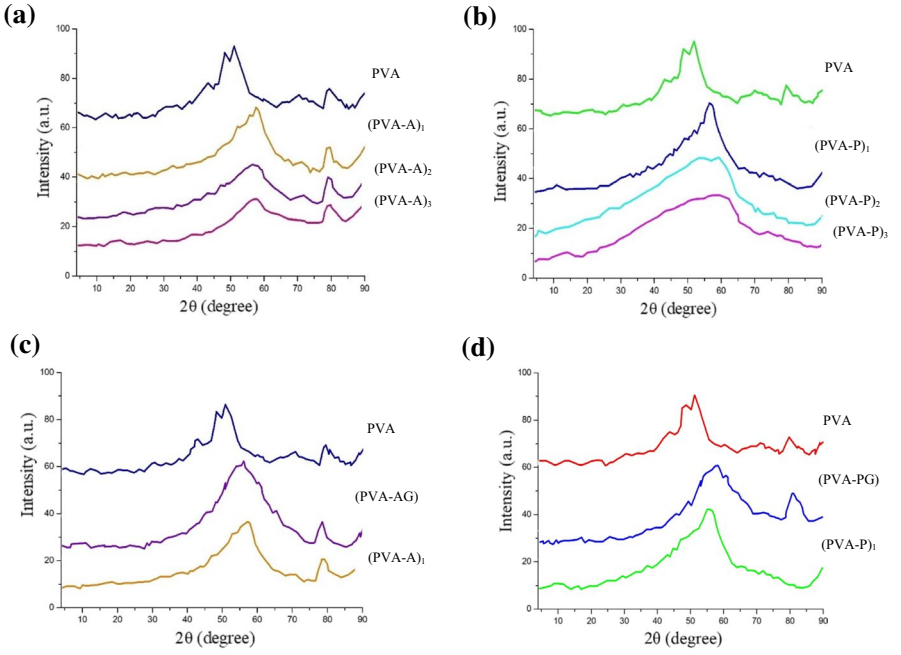

Fig. 3 X-ray diffraction pattern of **a** PVA, $(PVA\text{-}A)_{1–3}$, **b** PVA, $(PVA\text{-}P)_{1–3}$, **c** PVA, (PVA-AG), $(PVA\text{-}A)_1$ and **d** PVA, (PVA-PG), $(PVA\text{-}P)_1$

Table 1 Sol–gel fraction for the different membranes

Membrane code	Soluble fraction %				Gel fraction %			
	MeOH	DMF	DMSO	Water	MeOH	DMF	DMSO	Water
$(PVA\text{-}A)_1$	6	27	25	25	94	73	75	75
$(PVA\text{-}A)_2$	4	23	21	22	96	77	79	78
$(PVA\text{-}A)_3$	3	21	19	18	97	79	81	82
(PVA-AG)	2	17	16	12	98	83	84	88
$(PVA\text{-}P)_1$	19	29	28	27	81	71	72	73
$(PVA\text{-}P)_2$	17	25	23	23	83	75	77	77
$(PVA\text{-}P)_3$	15	23	21	20	85	77	79	80
(PVA-PG)	12	18	17	14	88	82	83	86

Table 2 Mean value of swelling ratio of different membranes with their relative standard deviations

Membrane code	Swelling ratio %							
	MeOH		DMF		DMSO		Water	
	Mean	RSD`%	Mean	RSD%	Mean	RSD%	Mean	RSD%
$(PVA\text{-}A)_1$	25.83	4.87	65.66	6.867	132.33	2.65	289.33	6.56
$(PVA\text{-}A)_2$	21.80	3.50	52.33	6.70	119	2.11	221.33	3.20
$(PVA\text{-}A)_3$	20.66	7.39	39.66	7.70	112.6	2.70	180.30	3.05
(PVA-AG)	17.16	4.45	31.66	3.28	76.33	4.58	102.33	2.03
$(PVA\text{-}P)_1$	53.33	4.68	229.66	7.03	557.33	4.68	667.66	2.70
$(PVA\text{-}P)_2$	49.66	6.15	216.33	6.03	551.66	4.53	652	3.23
$(PVA\text{-}P)_3$	46	5.75	200.3	5.24	535.33	3.02	639.66	2.84
(PVA-PG)	41.83	5.37	92.66	7.57	115.33	3.90	148.66	2.36

DMSO, THF, NMP, chloroform, acetone and methanol which indicated that the membranes had network structures which can be used in different applications.

Swelling measurements

The sol–gel fraction and swelling ratio values from swelling of membranes $(PVA\text{-}A)_{1-3}$, $(PVA\text{-}P)_{1-3}$, (PVA-AG) and (PVA-PG) at room temperature are shown in Tables 1 and 2 and Fig. 4, respectively. The presence of hydrophilic amide groups is known to increase the hydrophilicity of the system and increases the swelling ratios of the samples [51]. Table 1 shows the effects of monomers and cross-linking agent on the gel fraction of different membranes. From the data, it was observed that the gel fraction increases by increasing concentration of monomers and in the presence of glutaraldehyde. The highest gel fraction was observed in

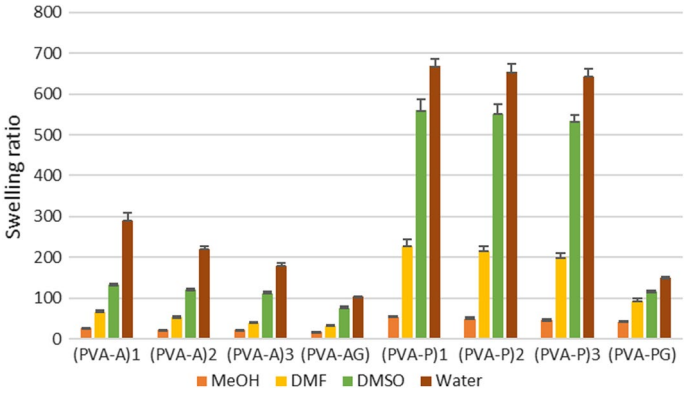

Fig. 4 Swelling ratio for the membranes $(PVA\text{-}A)_{1–3}$, (PVA-AG), $(PVA\text{-}P)_{1–3}$ and (PVA-PG)

the membrane (PVA-AG) reached 98% for methanol. From Table 2 and Fig. 4, the mean value of swelling ratios of the membranes was decreased as the concentration of the monomers increases due to the increase in the hydrophobicity and cross-linking of the membranes. The highest degree of swelling value for the membranes was observed with water rather than other aprotic solvents as result of the hydrogen bonding formation with the free hydroxyl groups of PVA. The results obtained from statistical analyses in Table 2 showed that relative standard deviation (RSD) of swelling ratio of different membranes was 2.11–7.7%.

It was noted that membranes $(PVA\text{-}P)_{1–3}$ had higher degree of swelling ratio than the membranes $(PVA\text{-}A)_{1–3}$, however the membranes $(PVA\text{-}A)_{1–3}$ and $(PVA\text{-}P)_{1–3}$ showed higher degree of swelling ratio than those produced in the presence glutaraldehyde (PVA-AG) and (PVA-PG), this was attributed to the increase in the degree of cross-linking and high thickness of the membranes (PVA-AG) and (PVA-PG) which decreased the degree of swelling capacity. It can be concluded that the membranes $(PVA\text{-}P)_{1–3}$ can be used for agriculture applications.

Morphology

The surface morphology of PVA and the new membranes was investigated using scanning electron microscopy (SEM) photographs at 30, 50 and 100 µm, respectively (Fig. 5). The structure morphology of the membranes $(PVA\text{-}A)_1$ and (PVA-AG) exhibited difference in the surface shape with appearance of porous structure than PVA. However, due to the presence of glutaraldehyde as cross-linker, there were more particles can be observed on the surface of membrane (PVA-AG) (Fig. 5a) [50]. The morphology for the membranes $(PVA\text{-}P)_1$ and (PVA-PG) had shapes as spots with rocks in the surface, beside more particles observed on the surface of the membrane (PVA-PG) which differs from the morphology of pure PVA, this confirmed the modifications of PVA (Fig. 5b).

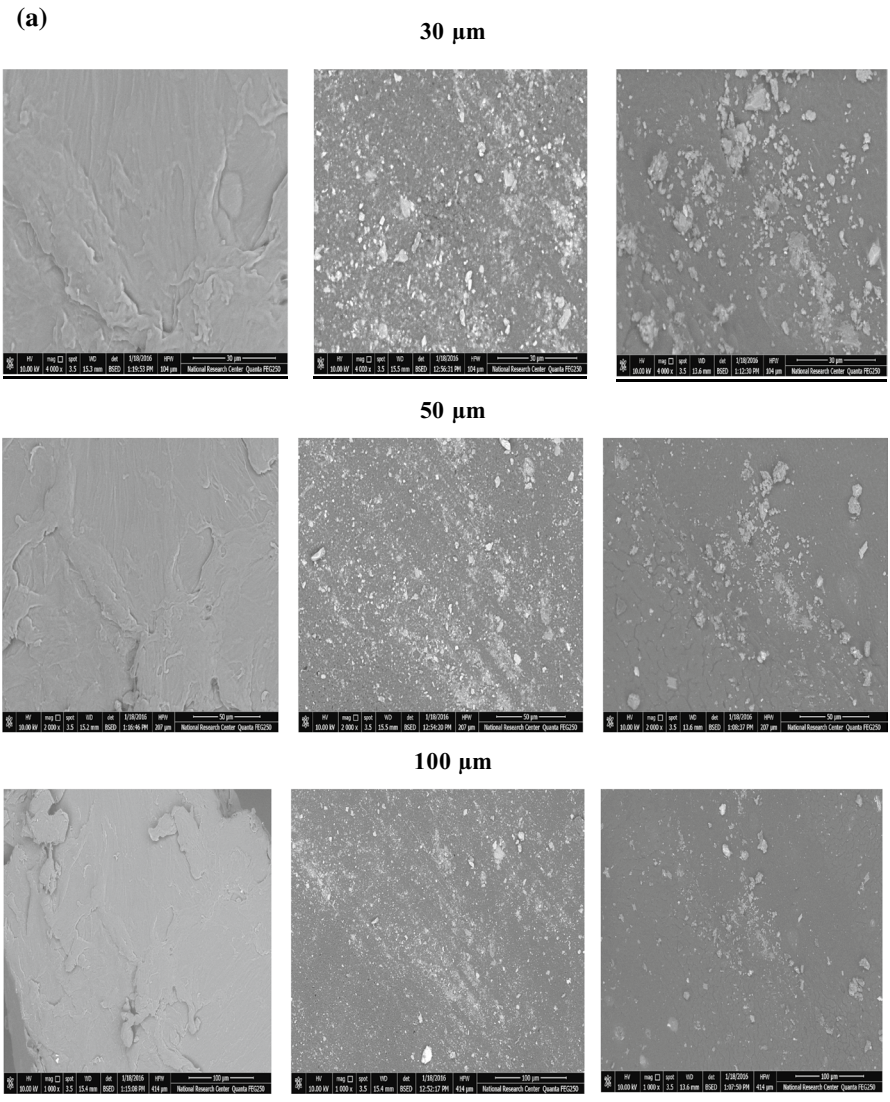

Fig. 5 SEM of **a** PVA, $(PVA\text{-}A)_1$, (PVA-AG) and **b** PVA, $(PVA\text{-}P)_1$, (PVA-PG) at 30, 50 and 100 µm, respectively

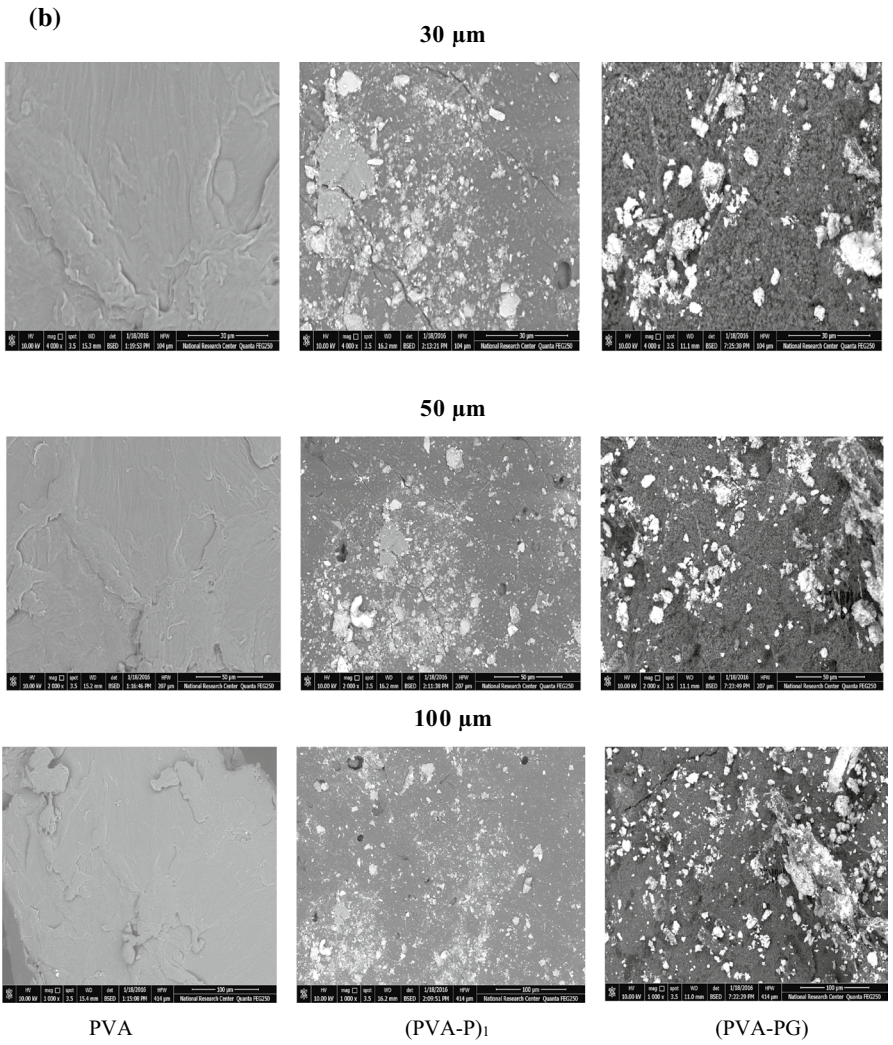

Fig. 5 (continued)

Evaluation of the prepared membranes for different applications

Antibacterial performance evaluation

The new membranes were screened for their antibacterial activities using the agar well diffusion technique [52]. The microorganisms used include (Gram-negative) *Escherichia coli* (ATCC-11229) and *Proteus* (ATCC-33420), and (Gram-positive) *Staphylococcus aureus* (ATCC-6538) and *B. subtilis* (ATCC-6633). For the antibacterial assay, a standard inoculum (105 CFU/ml) was float on the surface of sterile nutrient agar plates by a sterile glass spreader.

Table 3 Mean value of bacterial inhibition zone of PVA, different membranes and ciprofloxacin with their relative standard deviations

Compounds 50 g/ml	Inhibition zone diameter (mm)							
	Gram-negative				Gram-positive			
	E. coli		*Proteus*		*S. aureus*		*B. subtilis*	
	Mean	RSD%	Mean	RSD%	Mean	RSD%	Mean	RSD%
PVA	9.03	2.77	9.86	5.20	12.03	5.40	12.53	4.39
$(PVA\text{-}A)_1$	15.05	2.17	16.43	3.66	16.16	4.72	19.10	3.43
$(PVA\text{-}A)_2$	16.93	4.14	19.53	2.81	18.13	3.37	22.10	3.00
$(PVA\text{-}A)_3$	18.10	1.98	19.93	4.02	19.46	3.34	23.10	3.26
(PVA-AG)	22.96	3.70	25.46	2.55	24.90	3.43	30.56	1.96
$(PVA\text{-}P)_1$	12.03	2.91	13.50	5.92	13.46	4.82	15.50	3.87
$(PVA\text{-}P)_2$	13.43	2.61	15.03	5.65	14.53	4.47	17.56	3.42
$(PVA\text{-}P)_3$	14.46	3.11	15.46	5.49	15.50	5.16	18.06	4.44
(PVA-PG)	17.06	2.94	19.10	4.98	21.06	4.27	24.06	2.91
Ciprofloxacin	24.03	1.87	23.03	4.55	26.06	3.07	24.10	2.71

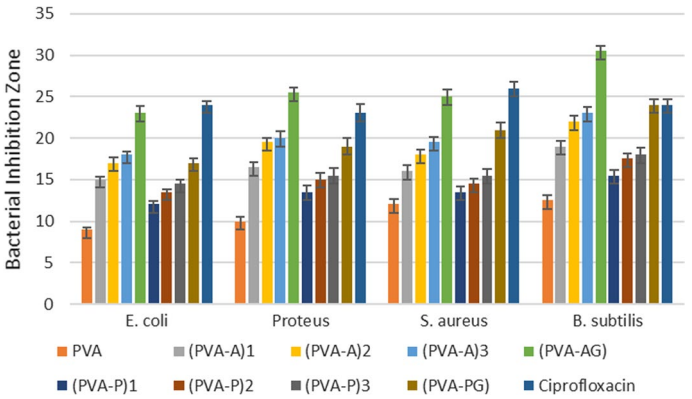

Fig. 6 Bacterial inhibition zone of PVA, $(PVA\text{-}A)_{1–3}$, (PVA-AG), $(PVA\text{-}P)_{1–3}$, (PVA-PG) and ciprofloxacin

Six-millimeter diameter wells were punched in the agar media and filled with 100 µL (500 µg/ml in DMSO) of the tested chemical compounds previously sterilized through 0.45 sterile membrane filter [53]. The plates were kept at room temperature for 1 h and then incubated at 37 °C for 24 h for bacteria.

The antimicrobial activities were evaluated by measuring the inhibition zone diameters. The values were reported as the mean ± SD. The mean values of bacterial inhibition zone of the membranes showed remarkable antibacterial activities against the microorganisms with a relative standard deviation of 1.87–5.92% as in Table 3.

Table 4 Mean value of percentage drug loading and release for different membranes with their relative standard deviations

Membrane code	% Drug loading		% Release	
	Mean	RSD%	Mean	RSD%
$(PVA\text{-}A)_1$	57.37	2.88	94.59	2.33
$(PVA\text{-}A)_2$	45.50	1.66	77.81	3.67
$(PVA\text{-}A)_3$	42.64	2.11	75.41	4.13
(PVA-AG)	35.14	4.43	72.55	3.36
$(PVA\text{-}P)_1$	48.45	2.68	79.00	3.74
$(PVA\text{-}P)_2$	40.46	2.10	77.68	3.46
$(PVA\text{-}P)_3$	37.12	2.42	69.93	4.39
(PVA-PG)	28.91	3.11	67.98	3.31

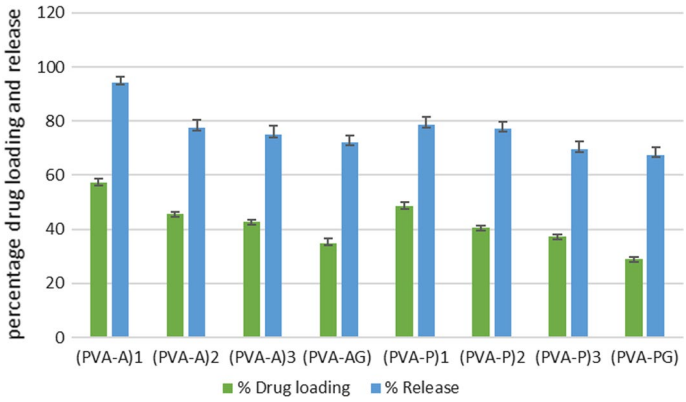

Fig. 7 The percentage drug loading and release for $(PVA\text{-}A)_{1–3}$, (PVA-AG), $(PVA\text{-}P)_{1–3}$ and (PVA-PG)

From Table 3 and Fig. 6, it can be concluded that the new membranes had high antibacterial effects compared to poly(vinyl alcohol) against both the tested bacteria (Gram-negative) *Escherichia coli* and *Proteus*, and (Gram-positive) *Staphylococcus aureus* and *B. subtilis* [50]. Membranes $(PVA\text{-}A)_{1–3}$ possess higher activity than the membranes $(PVA\text{-}P)_{1–3}$. However, membranes (PVA-AG) and (PVA-PG) showed the maximum antibacterial activity rather than the membranes formed in the absence of glutaraldehyde and antibacterial activities reached (22.9 and 25.46) toward (Gram-negative) *E. coli* and *Proteus* and (24.9, 30.56) toward (Gram-positive) *S. aureus* and *B. subtilis*, respectively, for the membrane (PVA-AG) due to the increase in the number of monomers which improved the activity toward both bacterial strains. Membrane (PVA-AG) was a potent antimicrobial agent due to its excellent antibacterial activity against (Gram-negative) *Proteus* and (Gram-positive) *B. subtilis* showed higher activity compared to standard antibiotic Ciprofloxacin. High antibacterial activity of membrane (PVA-AG) could be attributed to its highest thickness which makes the structure and chemistry of (Gram-negative) and (Gram-positive) bacteria more complex [54].

Drug loading and release of the membranes

The amount of percentage of loading and release of lidocaine (LD) for the membranes $(PVA\text{-}A)_{1–3}$, $(PVA\text{-}P)_{1–3}$, (PVA-AG) and (PVA-PG) was determined by post-loading process and is presented in Table 4 and Fig. 7.

The presence of heteroatoms (N, O) in the membranes was considered to increase the amount of percentage loading and release of lidocaine at high pH 7.4 by diffusion-gel swelling. The percentage loading and release of (LD) from the membranes decreases as the concentration of monomers increases due to the increase in the cross-linking of the membranes which decreased the space between macromolecular chains and decreases of water content [55–57]. It was noted also that membrane $(PVA\text{-}A)_1$ showed the highest percentage for lidocaine loading and release 57.37% and 94.59% with a relative standard deviation of 2.88% and 2.33%, respectively, however membranes $(PVA\text{-}A)_{1–3}$ had higher percentage for loading and release of (LD) than membranes $(PVA\text{-}P)_{1–3}$, moreover membranes $(PVA\text{-}A)_{1–3}$ and $(PVA\text{-}P)_{1–3}$ had a higher percentage than (PVA-AG) and (PVA-PG) due to cross-linking with glutaraldehyde. The data indicated that the drug release was inversely proportional to membrane thickness, as the thickness of membranes increased, the resistance of the membrane to water diffusion increased and the percentage of drug release decreased [58].

Metal ions uptake efficiency

The efficiency of the new membranes for the uptake of different metal ions such as (copper, cobalt and mercury) ions from aqueous systems was evaluated. The adsorption capacity values increased with increasing the contact time of immersion of the membranes up to 10 h (Table 5). This may be due to the increase in number of

Table 5 Effect of immersion time of different membranes and their efficiency on metal ions uptake

Membrane code	Immersion time (h)	Cu^{2+} (g/l)	Efficiency (%)	Co^{2+} (g/l)	Efficiency (%)	Hg^{2+} (g/l)	Efficiency (%)
$(PVA\text{-}A)_1$	0	2.0	–	2.0	–	2.0	–
	5	1.1	45	0.99	50.5	0.83	58.5
	10	1.0	50	0.71	64.5	0.61	69.5
(PVA-AG)	0	2.0	–	2.0	–	2.0	–
	5	0.96	52	0. 8	60	0.78	61
	10	0.71	64.5	0.61	69.5	0.54	73
$(PVA\text{-}P)_1$	0	2.0	–	2.0	–	2.0	–
	5	1.6	20	1.36	32	1.34	33
	10	1.36	32	1.2	40	1.05	47.5
(PVA-PG)	0	2.0	–	2.0	–	2.0	–
	5	1.34	33	1.04	48	0.99	50.5
	10	1.15	42.5	0.8	60	0.76	62

chelation between the metal ions and functional groups in the membranes. Data in Table 5 indicated that the efficiency of metal ions uptake of the membranes was found as $Hg^{2+} > Co^{2+} > Cu^{2+}$. It is suggested that the functional groups on the adsorbent had strong tendency to form complexes with Hg^{2+}better than other metal ions, this means that the surface-modified PVA membranes had high selectivity for Hg^{2+}[59].

Membrane $(PVA\text{-}A)_1$ exhibited high efficiency of Hg^{2+}uptake (69.5%), however, for membrane (PVA-AG) gave the highest efficiency 73% [49]. This could be due to the higher thickness of membrane (PVA-AG) than membrane $(PVA\text{-}A)_1$ which increase the number of pores gets and provide more active sites in the membrane for effective chelating of metal ions [60].

The data pointed to membranes containing aliphatic moiety in its structure $(PVA\text{-}A)_1$ and (PVA-AG) showed higher efficiency than membranes containing aromatic moiety in its structure $(PVA\text{-}P)_1$ and (PVA-PG). It is important to be noted that the highest efficiency of metal ions uptake for the membranes was revealed from the membranes prepared in the presence of glutaraldehyde due to increase in cross-linking. The 2 hydrogels $(PVA\text{-}A)_1$ and (PVA-AG) showed the highest metal ions uptake efficiency was tested for 24 h immersion time and it exhibited that the adsorption capacity was constant after 24 h immersion time. These results showed that these membranes may be potential for metal ions removal from aqueous systems.

Desorption and reusability of the prepared membranes

The stability of the prepared membranes in water treatment application can be evaluated by immersing it in solution composed of mixture from 0.1 M HCl to 0.1 M EDTA and stirred for 4 h, then washed with distilled water several times till the pH of water solution became neutral. The adsorption efficiency of metal ions by each cross-linked membrane after the second cycle was about 10% lower efficiency than its original.

The adsorption efficiency of the prepared membranes was remained about 70% by the 6 cycle [61]. This indicated that the prepared membranes can be used for water treatment from heavy metal ions for 6 cycle.

Conclusions

In this research, different cross-linked membranes $(PVA\text{-}A)_{1–3}$, $(PVA\text{-}P)_{1–3}$, (PVA-AG) and (PVA-PG) were synthesized successfully through the reaction between PVA and different concentrations of heterocyclic compounds [*N*,*N*′-bi-*α*-azido succinimide (A) or *N*-phthalimido-*α*-azido succinimide (P)] and glutaraldehyde (G), respectively. The new membranes were characterized using various tools for analysis. Swelling behavior of the new membranes decreased and gel fraction increased as heteroatoms and carbon chain incorporated in membranes due to the network structures. (PVA-AG) membrane showed the highest gel fraction while $(PVA\text{-}P)_{1–3}$ membranes exhibited the highest swelling capacity in different solvents. The thermal stability of membranes was enhanced after the cross-linking with (G). Hence, the surface morphology study of the membranes revealed particles, rocks

and porous structure compared to smooth structure of PVA which confirmed the chemical modification of PVA with the monomers. Based on XRD results, the crystallinity was decreased with increasing the concentration of the monomers in the $(PVA\text{-}A)_{1-3}$ and $(PVA\text{-}P)_{1-3}$ membranes, however the highest crystallinity was observed after cross-linking with glutaraldehyde (PVA-AG) and (PVA-PG). (PVA-AG) showed superior activity compared to the reference antibiotic Ciprofloxacin. Furthermore, the in vitro release profiles showed sustained released for LD reached 94.59% represented by $(PVA\text{-}A)_1$ membrane which displayed the highest LD loaded percent (57.37%). Moreover, (PVA-AG) membrane revealed the highest adsorption efficiency of metal ions [Cu^{2+}, Co^{2+} and Hg^{2+}]. It can be concluded that the chemical modification of PVA with heterocyclic compounds [*N*,*N*′-bi-*α*-azido succinimide (A) and *N*-phthalimido-*α*-azido succinimide (P)] improved its physicochemical properties and enhanced its antibacterial activity, drug delivery efficiency and metal ions adsorption capacity from aqueous medium.

Acknowledgements The authors gratefully acknowledge the Chemistry Department, Faculty of Women for Art, Science and Education, Ain Shams University, for its support.

Funding Open access funding provided by The Science, Technology & Innovation Funding Authority (STDF) in cooperation with The Egyptian Knowledge Bank (EKB).

Declarations

Conflict of interest The authors declare that they have no conflict of interest.

References

1. Zhang S, Yu H, Chen Q, Hu H, Yingxu SY, Chen J, Cao Y, Xiang M (2020) Influence of pentaerythritol on the properties of polyvinyl alcohol films for the polarizers. J Polym Res 27:31
2. Yihun FA, Ifuku S, Saimoto H, Yihun DA (2021) Thermo-mechanically improved polyvinyl alcohol composite films using maleated chitin nanofibers as nano-reinforcement. Cellulose 28: 2965–2980
3. Ren G, Xu X, Liu Q, Cheng J, Yuan X, Wu L, Wan Y (2006) Electrospun poly(vinyl alcohol)/glucose oxidase biocomposite membranes for biosensor applications. React Funct Polym 66:1559–1564
4. Kang GD, Cao YM (2012) Development of antifouling reverse osmosis membranes for water treatment: a review. Water Res 46:584–600
5. Yeum JH, Ji BC, Noh SK, Jeon HY, Kwak JW, Lyoo WS (2004) Effect of syndiotacticity on the morphology of water-soluble low molecular weight poly(vinyl alcohol) by solution copolymerization of vinyl pivalate/vinyl acetate in tetrahydrofuran and saponification. Polymer 45:4037–4043
6. Nagarkar R, Patel J (2019) Polyvinyl alcohol: a comprehensive study. ASPS 3(4):34–44
7. Guirguis OW, Moselhey MTH (2012) Thermal and structural studies of poly(vinyl alcohol) and hydroxypropyl cellulose blends. Nat Sci 4(1):57–67

8. Zadeh SN, Rajabnezhad S, Zandkarimi M, Dahmardeh S, Mir L (2017) Mucoadhesive microspheres of chitosan and polyvinyl alcohol as a carrier for intranasal delivery of insulin: in vitro and in vivo studies. MOJ Bioequiv Availab 3(2): 00030
9. Kermani AS, Mirzaee M, Moghaddam MG (2016) Polyvinyl alcohol/polyaniline/ZnO nanocomposite: synthesis, characterization and bactericidal property. Adv Biol Charact Bactericidal Chem 6:1–11
10. Hassan CM, Peppas NA (2000) Structure and applications of poly(viny1 alcohol) hydrogels produced by conventional crosslinking or by freezing/thawing methods. Adv Polym Sci 153:37–65
11. Gajra B, Pandya SS, Vidyasagar G, Rabari H, Dedania RR, Rao S (2012) Polyvinyl alcohol hydrogel and its pharmaceutical and biomedical applications. Int J Pharm Res 4:20–26
12. Teodorescu M, Bercea M, Morariu S (2019) Biomaterials of PVA and PVP in medical and pharmaceutical applications: perspectives and challenges. Biotechnol Adv 37:109–131
13. Zanela J, Bilck AP, Reis MO, Grossmann MVE, Yamashita F (2020) Modified starches on the properties of extruded biodegradable materials of starch and polyvinyl alcohol. J Polym Environ 28(12):3211–3220
14. Pei C, Ueda T, Zhu J (2020) Investigation of the effectiveness of graphene/polyvinyl alcohol on the mechanical and electrical properties of cement composites. Mater Struct 53:66
15. Gadhave RV, Mahanwar PA, Gadekar PT, Kasbe PS (2020) A study on the effect of starch–polyvinyl alcohol blends by addition of citric acid and boric acid for enhancement in performance properties of polyvinyl acetate-based wood adhesive. J Indian Acad Wood Sci 17(1):9–20
16. Bal T, Swain S (2020) Microwave assisted synthesis of polyacrylamide grafted polymeric blend of fenugreek seed mucilage-polyvinyl alcohol (FSM-PVA-g-PAM) and its characterizations as tissue engineered scaffold and as a drug delivery device. DARU J Pharm Sci 28:33–44
17. Conte A, Buonocore GG, Sinigaglia M, Nobile MAD (2007) Development of immobilized lysozyme based active film. J Food Eng 78:741–745
18. Hasimi A, Stavropoulou A, Papadokostaki KG, Sanopoulou M (2008) Transport of water in polyvinyl alcohol films: effect of thermal treatment and chemical crosslinking. Eur Polym J 44:4098–4107
19. Mansur HS, Mansur AAP (2005) Small angle X-ray scattering, FTIR and SEM characterization of nanostructured PVA/TEOS hybrids by chemical crosslinking. Mater Res Soc Symp Proc 873:20–25
20. Park JS, Park JW, Ruckenstein E (2001) On the viscoelastic properties of poly(vinyl alcohol) and chemically crosslinked poly(vinyl alcohol). J Appl Polym Sci 82:1816–1823
21. Jamnongkan T, Wattanakornsiri A, Wachirawongsakorn P, Kaewpirom S (2014) Effects of crosslinking degree of poly(vinyl alcohol) hydrogel in aqueous solution: kinetics and mechanism of copper(II) adsorption. Polym Bull 71:1081–1100
22. Jahan F, Mathad RD (2017) Mechanical studies on chitosan/PVA blend with calcium chloride as ionic crosslinker. Int J Adv Sci Eng Technol 4:31–34
23. Zhen W, Feng Y, Hongchang P, Jianxin L, Zhenyu C, Benqiao H (2018) Antibacterial and environmentally friendly chitosan/polyvinyl alcohol blend membranes for air filtration. Carbohydr Polym 198:241–248
24. Maruhashi M (1992) In poly(vinyl alcohol), Ch.7, II; Finch, CA, Ed. Wiley, New York
25. Moritani T, Kajitani K (1997) Functional modification of poly(vinyl alcohol) by copolymerization: 1. Modification with carboxylic monomers. Polymer 38:2933
26. Petreus O, Bubulac TV, Hamciuc C (2005) Synthesis and characterization of new polyesters with enhanced phosphorus content. Eur Polym J 41:2663–2670
27. Pellon RF, Carrasco R, Rodes L (1993) Synthesis of *N*-phenylanthranilic acids using water as solvent. Synth Commun 23:1447–1453
28. Saeed RS, Matty FS, Samir AH (2019) Chemical modification of PVA with four, five and seven heterocyclic compounds and study anticancer activity. J Pharm Sci Res 11(3):733–740
29. Aminabhavi TM, Nadagouda MN, More UA, Joshi SD, Venkatrao HK, Malleshappa NN (2015) Controlled release of therapeutics using interpenetrating polymeric networks. Expert Opin Drug Deliv 12:669–688
30. Praveen BK, Lata SM, Aminabhavi TM (2014) Novel blend microspheres of cellulose triacetate and bee wax for the controlled release of nateglinide. J Ind Eng Chem 20:397–404
31. Feng JL, Yue CY, Chian KS (2006) Synthesis and characterization of the bismaleimides containing aliphatic-ether chain for microelectronics application. e-Polymers no 044: 1–11
32. Sava M (2013) Preparation and characterization of bismaleimide monomers with various structures. Des Monomers Polym 16(1):14–24

33. Kandile NG, Nasr AS (2009) Environment friendly modified chitosan hydrogels as a matrix for adsorption of metal ions, synthesis and characterization. Carbohydr Polym 78:753–759
34. Kandile NG, Nasr AS (2011) Hydrogels based on a three-component system with potential for leaching metals. Carbohydr Polym 85:120–128
35. Kandile NG, Nasr AS (2011) New polyamides and polyesteramides incorporated with bis (carboxy-substituted) hydrazines: synthesis and characterization. J Appl Polym Sci 122:1152–1161
36. Kandile NG, Nasr AS (2014) New hydrogels based on modified chitosan as metal biosorbent agents. Int J Biol Macromol 64:328–333
37. Kandile NG, Mohamed HM, Mohamed MI (2015) New heterocycle modified chitosan adsorbent for metal ions (II) removal from aqueous systems. Int J Biol Macromol 72:110–116
38. Kandile NG, Mohamed MI, Zaky HT, Nasr AS, Ali YG (2021) Quinoline anhydride derivatives cross-linked chitosan hydrogels for potential use in biomedical and metal ions adsorption. Polym Bull. https://doi.org/10.1007/s00289-021-03633-w
39. Awad WI, Ismail MF, Kandile NG (1976) Reaction of hydrazoic acid and diazo compounds with *N*,*N*′-bimaleimide and biisomaleimide. Egypt J Chem 19:251–255
40. Awad WI, Kandile NG, Ismail MF (1979) Action of Grignard reagents on mixed biimides. J Prakt Chem Band Heft 321:8–12
41. Alla SG, El-Din HMN, El-Naggar AWM (2007) Structure and swelling-release behaviour of poly(vinyl pyrrolidone) (PVP) and acrylic acid (AAc) copolymer hydrogels prepared by gamma irradiation. Eur Polym J 43:2987–2998
42. Lin CL, Chiu WY, Lee CF (2005) Thermal/pH-sensitive core–shell copolymer latex and its potential for targeting drug carrier application. Polymer 46(23):10092–10101
43. Aroguz AZ, Baysal K, Tasdelen B, Baysal BM (2011) Preparation, characterization, and swelling and drug release properties of a crosslinked chitosan-polycaprolactone gel. J Appl Polym Sci 119:2885–2894
44. Husain T, Ansari M, Ranjha NM (2013) Chemically cross-linked poly (acrylic-*co*-vinylsulfonic) acid hydrogel for the delivery of isosorbide mononitrate. World Sci J 2013:1–9
45. Rudra R, Kumar V, Kundu PP (2015) Acid catalysed cross-linking of polyvinyl alcohol (PVA) by glutaraldehyde: effect of crosslink density on the characteristics of PVA membranes used in single chambered microbial fuel cells. RSC Adv 5:83436–83447
46. Jia X, Li Y, Zhang B, Cheng Q, Zhang S (2008) Preparation of poly(vinyl alcohol)/kaolinite nanocomposites via in situ polymerization. Mater Res Bull 43:611–617
47. Lee SY, Mohan DJ, Kang IA, Doh GH, Lee S, Han SO (2009) Nanocellulose reinforced PVA composite films: effects of acid treatment and filler loading. Fibers Polym 10:77–82
48. Zhang J, Lei W, Liu D, Wang X (2017) Synergistic influence from the hybridization of boron nitride and graphene oxide nanosheets on the thermal conductivity and mechanical properties of polymer nanocomposites. Compos Sci Technol 151:252–257
49. Chen Q, Zhu L (2012) PVA/PVAm hydrogel membranes for removal of metal ions from aqueous solution. Appl Mech Mater 130–134:1507–1510
50. Suganthi S, Vignesh S, Sundar JK, Raj V (2020) Fabrication of PVA polymer films with improved antibacterial activity by fine-tuning via organic acids for food packaging applications. Appl Water Sci 10:100
51. Okudan A, Altay A (2019) Investigation of the effects of different hydrophilic and hydrophobic comonomers on the volume phase transition temperatures and thermal properties of N-Isopropylacrylamide based hydrogels. Int J Polym Sci 2019:1–12
52. Ahmad S, Rathish IG, Bano S, Alam MS, Javed K (2010) Synthesis and biological evaluation of some novel 6-aryl-2-(p-sulfamylphenyl)-4,5-dihydropyridazin-3(2H)-ones as anti-cancer, antimicrobial, and anti-inflammatory agents. J Enzym Inhib Med Chem 25:266–271
53. Karthikeyan SM, Prasad JD, Mahalinga M, Holla SB, Kumari SN (2008) Antimirobial studies of 2,4-dihloro-5-fluorophenyl containing oxadiazoles. Eur J Med Chem 43:25–31
54. Li S, Zhang R, Xie J, Sameen DE, Ahmed S, Dai J, Qin W, Li S, Liu Y (2020) Electrospun antibacterial poly(vinyl alcohol)/Ag nanoparticles membrane grafted with 3,3′,4,4′-benzophenone tetracarboxylic acid for efficient air filtration. Appl Surf Sci 533:147516
55. Canal T, Peppas NA (1989) Correlation between mesh size and equilibrium degree of swelling of polymeric networks. J Biomed Mat Res 23:1183–1193
56. Peppas NA, Bures P, Leobandung W, Ichikawa H (2000) Hydrogels in pharmaceutical formulations. Eur J Pharm Biopharm 50:27–46

57. Zhao P, Jiang H, Pan H, Zhu K, Chen W (2007) Biodegradable fibrous scaffolds composed of gelatin coated poly(ε-caprolactone) prepared by coaxial electrospinning. J Biomed Mat Res A 83A:372–382
58. Nokhodchi A, Momin MN, Shokri J, Shahsavari M, Rashidi PA (2008) Factors affecting the release of nifedipine from a swellable elementary osmotic pump. Drug Deliv 15:43–48
59. Tian Y, Wu M, Liu R, Li Y, Wang D, Tan J, Wu R, Huang Y (2011) Electrospun membrane of cellulose acetate for heavy metal ion adsorption in water treatment. Carbohydr Polym 83:743–748
60. Sangeetha K, Angelin Vinodhini P, Sudha PN, Alsharani Faleh A, Sukumaran A (2019) Novel chitosan based thin sheet nanofiltration membrane for rejection of heavy metal chromium. Int J Biol Macromol 132:939–953
61. Zulfiqar M, Lee SY, Mafize AZ, Abdul Kahar NAM, Johari KH, Rabat NE (2020) Efficient removal of Pb(II) from aqueous solutions by using oil palm bio-waste/MWCNTs reinforced PVA hydrogel composites: kinetic, isotherm and thermodynamic modeling. Polymers 12:430